Journal of Materials Chemistry A

COMMUNICATION

View Article Online
View Journal | View Issue

Cite this: J. Mater. Chem. A, 2014, 2, 6348

Received 30th January 2014
Accepted 3rd March 2014

DOI: 10.1039/c4ta00535j

www.rsc.org/MaterialsA

A high molecular weight triisopropylsilylethynyl (TIPS)-benzodithiophene and diketopyrrolopyrrole-based copolymer for high performance organic photovoltaic cells†

Ji-Hoon Kim,[a] Minjung Lee,[b] Hoichang Yang[b] and Do-Hoon Hwang*[a]

A high-molecular-weight conjugated polymer consisting of alternating TIPS-substituted benzo[1,2-*b*:4,5-*b*′]dithiophene (BDT) and diketopyrrolo[3,4-*c*]pyrrole (DPP) was synthesized by Suzuki cross-coupling and characterized for use in high performance OPVs. Good structural order, self-assembly in spun-cast films, and carrier mobility were observed. PTIPSBDT–DPP showed an OFET hole mobility of up to 0.12 $cm^2 V^{-1} s^{-1}$. Power conversion efficiencies of up to 8.0% were demonstrated for OPV devices.

One of the most important issues for enhancing the power conversion efficiency (PCE) of organic photovoltaic cells (OPVs) has been the development of π-conjugated polymers that exhibit broad visible wavelength absorption, high charge carrier mobility (μ_{FET}), suitable energy level matching of frontier orbitals with those of the electron acceptor, and appropriate chain orientation that form an optimum pathway for the charge carriers to the electrodes. Creating bulk heterojunction (BHJ) morphologies containing nanometer-sized, interconnected, and π-conjugated domains of both the electron donors (D) and acceptors (A) is also crucial for photovoltaic performance. The optimization of π-conjugation along the polymer backbone *via* crystallization assists efficient charge separation. High molecular weight (M_n) and crystalline organic semiconductors are important for achieving such morphologies.[1]

Recently, diketopyrrolo[3,4-*c*]pyrrole (DPP) has emerged as a promising A building block for low band gap D–A conjugated polymers for optoelectronic applications, such as organic field-effect transistors (OFETs) and OPVs, because of its strong interchain π–π interactions and its highly electron accepting nature.[2]

A series of D–A type copolymers comprising benzo[1,2-*b*:4,5-*b*′]dithiophene (BDT) and DPP has been synthesized by many groups. In particular, Yang and co-workers reported highly efficient OPVs based on a low band gap conjugated copolymer (PBDTT–DPP), with alternating 4,8-bis(5-(2-ethylhexyl)thiophene-2-yl)-benzo[1,2-*b*;3,4-*b*]dithiophene (BDTT) and DPP, yielding a maximum PCE of 6.5%.[3]

As a BDT derivative, we have focused on triisopropylsilylethynyl (TIPS)-substituted BDT (TIPSBDT)-based polymers with HOMO energy levels below −5.50 eV and high open-circuit voltages (V_{oc}) above 0.90 V that result from the electron-withdrawing carbon–carbon triple bond in the bulky and highly solubilizing TIPS side moieties. As D–A copolymers, TIPSBDT and benzotriazole (DTBTz)-based polymers with medium band gaps showed excellent crystallinities in BHJ thin films with [6,6]-phenyl C_{71}-butyric acid methyl ester ($PC_{71}BM$), yielding high PCEs in the OPVs.[4] Li and co-workers also reported a low band-gap conjugated polymer consisting of TIPSBDT and thiazolothiazole derivative (PBDTTT–TIPS), and the polymer showed relatively high mobility, V_{oc} value, and PCEs.[5]

Here, we report a novel type of low band gap conjugated polymer (PTIPSBDT–DPP) containing DPP and TIPSBDT, and successfully demonstrate its excellent electrical properties in both OFETs and OPVs. The Stille cross-coupling reaction has been widely used for the copolymerization of BDT and DPP derivatives, yielding copolymers with number average molecular weights (M_n) ranging from 20 000 to 40 000 g mol^{-1}.[3] Additionally, Suzuki cross-coupling polymerization reactions have been used for the DPP-based conjugated polymers; K_2CO_3 and K_3PO_4 are generally used as bases. Ober *et al.* reported that high-M_n conjugated polymers could be achieved through a Suzuki coupling polymerization reaction with tetraethylammonium hydroxide (Et_4NOH) as a base, with M_n ranging from 120 000 to 150 000 g mol^{-1}.[6]

As shown in Fig. 1a, PTIPSBDT–DPP was synthesized by Suzuki cross-coupling polymerization and subsequently purified (see the Experimental section). The polymerization was

[a]Department of Chemistry, Chemistry Institute for Functional Materials, Pusan National University, Busan 609-735, Korea. E-mail: dohoonhwang@pusan.ac.kr; Fax: +82 (51) 516 7421; Tel: +82 (51) 510 2232

[b]Department of Advanced Fiber Engineering, Optoelectronic Hybrids Research Center, Inha University, Incheon 402-751, Korea

† Electronic supplementary information (ESI) available. See DOI: 10.1039/c4ta00535j

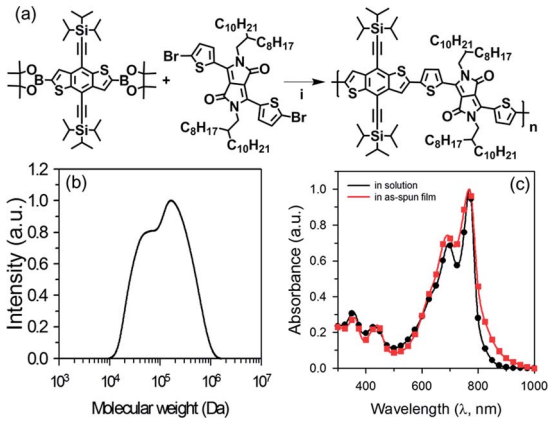

Fig. 1 (a) Synthetic scheme for the PTIPSBDT–DPP copolymer: (i) $Pd(PPh_3)_4$, Bu_4NBr, toluene, aq. Et_4NOH (20 wt%), 110 °C, 24 h, Ar. (b) GPC profile of PTIPSBDT–DPP used in this study. (c) Normalized UV-vis absorption spectra of PTIPSBDT–DPP in dilute $CHCl_3$ solution and as the as-spun film.

carried out by reacting 2,6-bis(4,4,5,5-tetramethyl-1,3,2-dioxaborolan-2-yl)-4,8-bis(triisopropylsilylethynyl)-benzo[1,2-*b*:4,5-*b*′]-dithiophene (TIPSBDT) and 5-dioctyldodecyl-3,6-bis(5-bromothiophen-2-yl)pyrrolo[3,4-*c*]pyrrole-1,4-dione (DPP) in toluene with $Pd(PPh_3)_4$ as the catalyst and aqueous Et_4NOH as the base. The resulting polymer was then purified by successive Soxhlet extractions with acetone, hexane, and chloroform as solvents, followed by column chromatography with a chloroform–THF mixture as the eluent. The gel permeation chromatography (GPC) curve related to the hydrodynamic volume of the polymer dissolved in *o*-dichlorobenzene corresponded to an average M_n of 76 000 g mol^{-1} (polydispersity index (PDI) = ~2.50) (Fig. 1b), potentially leading to longer intramolecular conjugation than other reported BDT–DPP-based conjugated polymers.[3] Thermogravimetric analysis showed that the polymer had excellent thermal stability, with only 5% weight loss even at 400 °C (Fig. S1a in the ESI†).[7] Additionally, the polymer powder clearly showed a semi-crystalline behavior with melting (T_m) and crystallization (T_c) temperatures of 216.8 and 206.3 °C, respectively, as determined by differential scanning calorimetry (DSC) profiles (Fig. S1b in the ESI†).

Fig. 1c presents the ultraviolet-visible (UV-vis) absorption spectra of PTIPSBDT–DPP in chloroform solution and as the as-spun film. For both samples, broad absorption bands ranging from 600 to 900 nm (near-infrared region) showed maximum intensities at 770 nm, originating from the D–A conjugated backbone structure. The absorption spectra of the PBDTT–DPP solution and the thin film were quite similar except slight red shift of the onset position in the solid film state. The optical band gap of the PBDTT–DPP film was measured to be 1.44 eV from its absorption onset wavelength (λ = 860 nm) which is approximately 20 nm redshift from that of the typical BDT and DPP based polymer, poly{2,6′-4,8-di(5-ethylhexylthienyl)benzo-[1,2-*b*:3,4-*b*]dithiophene-*alt*-5-dibutyloctyl-3,6-bis(thiophene-2-yl)pyrrolo[3,4-*c*]pyrrole} (PBDTT–DPP).[3] This was attributed to the additional extension of π-conjugation by the triple bonds in the TIPS side groups. The sp carbon with high electron affinity in PTIPSBDT–DPP also contributed to the deeper HOMO level (−5.44 eV) than that of PBDTT–DPP (−5.40 eV), as determined by cyclic voltammetry analysis (Fig. S2 in the ESI†). The LUMO energy level of PTIPSBDT–DPP was estimated to be −4.00 eV, providing a suitable offset between the LUMO level of $PC_{71}BM$ (−4.30 eV) to ensure efficient charge separation. Based on these results, it was expected that the high-M_n PTIPSBDT–DPP could grow into π-conjugated crystal structures during solution film casting.[1] Table S1† summarizes the polymerization results and thermal properties of the copolymers.

The electrical properties of PTIPSBDT–DPP were first investigated in organic field-effect transistors (OFETs). Films with thicknesses of 50 nm were spun-cast on monolayer-thick dimethylchlorosilane-terminated polystyrene ($PS–Si(CH_3)_2Cl$) grafted to SiO_2 (referred to as PS brush-SiO_2) dielectrics from 0.5 vol% chlorobenzene (CB) solution (see the Experimental section).[8] Some spun-cast films were post-treated at different annealing temperatures (T_As; 100, 120, 150, or 200 °C) for 10 min. To fabricate a top-contacted electrode OFET (Fig. 2a), Au electrodes were finally evaporated onto these PTIPSBDT–DPP films through a shadow mask. Fig. 2b shows typical drain current–gate voltage (I_D–V_G) transfer curves of the OFETs containing spun-cast PTIPSBDT–DPP films before and after thermal annealing at 100 °C (see Fig. S4 and S5 in the ESI†). The electrical performance of all the OFETs is summarized in Table S2.† In the OFET, the as-spun PTIPSBDT–DPP film on the organo-compatible PS brush-SiO_2 dielectric showed a much higher μ_{FET} value (0.06 cm^2 V^{-1} s^{-1}) than that of the same film on an untreated SiO_2 dielectric (0.008 cm V^{-1} s^{-1}), which contained many surface charge-trap sites (Fig. S4 in the ESI†).[9] Additionally, the electrical performance of OFETs containing T_A-annealed PTIPSBDT–DPP films was improved: specifically,

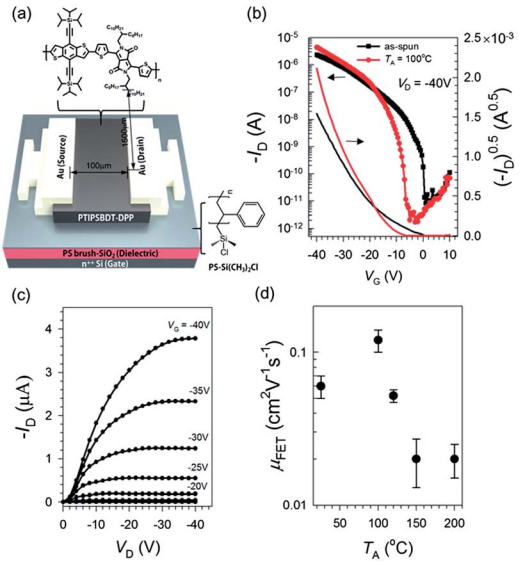

Fig. 2 (a) Scheme of a top-contacted electrode OFET containing a PTIPSBDT–DPP film. (b) I_D–V_G transfer curves of OFETs containing spun-cast PTIPSBDT–DPP films before and after annealing at 100 °C. (c) I_D–V_D output curves of the T_A = 100 °C annealed sample. (d) T_A-dependent variations in μ_{FET}.

the $T_A = 100$ °C sample, showing clear p-type transistor characteristics (Fig. 2c), yielded the highest μ_{FET} (0.12 $cm^2 V^{-1} s^{-1}$) as well as a high on–off current ratio (I_{ON}/I_{OFF}) that exceeded 10^5. Above $T_A = 100$ °C, however, the μ_{FET} values of the T_A-annealed films decreased gradually below the initial value, to 0.02 $cm^2 V^{-1} s^{-1}$ (Fig. 2d).

It is well known that π-conjugated film morphologies of solution-processed organic semiconductors significantly affect their electrical properties in OFETs. The topography of the 100 °C annealed film determined by atomic force microscopy (AFM) showed a highly interconnected morphology of regularly phase-separated PTIPSBDT–DPP nanorods with a lateral width of 22–25 nm and a length of 300–500 nm (Fig. S5 in the ESI†). Since all the PTIPSBDT–DPP OFETs showed enough charge-carrier mobility to achieve highly efficient OPVs (*i.e.*, comparable to or exceeding 10^{-3} $cm^2 V^{-1} s^{-1}$), the interconnected nanofibril network of PTIPSBDT–DPP was expected to yield efficient charge extraction and a good fill factor (FF) in OPV applications.

BHJ OPVs were fabricated and characterized to investigate the photovoltaic properties of PTIPSBDT–DPP (see Experimental section). The performance of the prepared OPVs was strongly affected by the processing parameters, including the choice of solvent, blend ratio of the polymer and $PC_{71}BM$, and the processing additive effect (see ESI†). To optimize the PTIPSBDT–DPP:$PC_{71}BM$ blend ratio in the BHJ films, active layers were spun-cast from CB solutions with blend ratios of 1 : 1, 1 : 2, and 1 : 3 w/w. Current density–voltage (*J–V*) curves of the OPVs were measured under AM 1.5 G illumination (100 mW cm^{-2}) (Fig. S6 in the ESI†). It was found that the BHJ OPV containing the 1 : 2 w/w PTIPSBDT–DPP:$PC_{71}BM$ blend film showed the maximum PCE value of up to 6.29%, a V_{oc} of 0.76 V, a J_{sc} of 14.52 mA cm^{-2}, and a FF of 0.57.

Next, we investigated the effects of introducing small amounts of 1.8-diiodooctane (DIO) to the CB, and the binary solvents were used to further improve the photovoltaic performance of the 1 : 2 w/w PTIPSBDT–DPP:$PC_{71}BM$ blend film. As expected, the photovoltaic performance of the PTIPSBDT–DPP:$PC_{71}BM$ blend system could be significantly enhanced by controlling the DIO volume in the binary solvent.

Fig. 3a and b show the *J–V* and external quantum efficiency (EQE) curves of OPVs containing 1 : 2 w/w PTIPSBDT–DPP:$PC_{71}BM$ blend films fabricated from the binary solvents, respectively. The resulting OPV characteristics are summarized in Table 1. A 3 vol% DIO-assisted blend film yielded the highest PCE value of 8.00% in an OPV, with a V_{oc} of 0.76 V, a J_{sc} of 16.21 mA cm^{-2}, and a FF of 0.65. Similar to other BDT–DPP copolymers, all the measured PTIPSBDT–DPP:$PC_{71}BM$ OPVs exhibited small variations in V_{oc}. The J_{sc} values were also calculated by integrating the EQE profiles with the AM 1.5 G reference spectrum to evaluate the accuracy of the measurements: the J_{sc} values obtained *via* integration and the *J–V* measurements were quite similar. The spectral responses of the OPV devices showed that photons with λ ranging from 350 to 850 nm contributed mainly to the EQE: specifically, the EQE could increase up to 66% at 500 nm.

To clarify the origin of the improvement in the OPVs, the binary solvent-dependent crystal morphologies and crystal

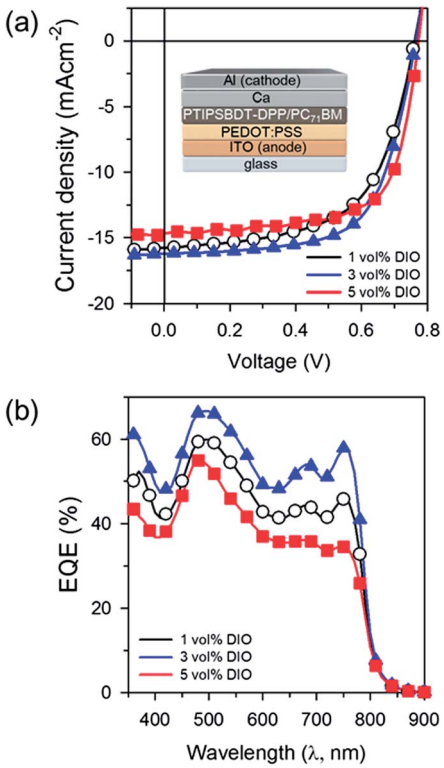

Fig. 3 (a) *J–V* curves and (b) EQE spectra of OPVs containing DIO-assisted spun-cast 1 : 2 w/w PTIPSBDT–DPP:$PC_{71}BM$ blend films spun-cast from binary solvents containing 1, 3, and 5 vol% DIO in CB. (The inset in (a) represents a scheme of the OPV geometry containing ITO/PEDOT:PSS/PTIPSBDT–DPP:$PC_{71}BM$/Ca/Al layers, with an active cell area of 9 mm^2.)

structures of the semiconducting films in the OPVs were investigated by atomic force microscopy (AFM), transmission electron microscopy (TEM), and two-dimensional (2D) grazing-incidence X-ray diffraction (GIXD) analyses. Fig. 4 shows AFM topographies and 2D GIXD patterns of the PTIPSBDT–DPP film and PTIPSBDT–DPP:$PC_{71}BM$ blend films spun-cast from either CB alone or the binary solvent system. AFM topography of the as-spun PTIPSBDT–DPP film showed a nanoporous mesophase structure (pore diameter: 20–25 nm) between amorphous and nanocrystalline, without any clear crystal features (Fig. 4a). Additionally, it was found that the copolymer had good compatibility with $PC_{71}BM$, forming a homogeneously blended (1 : 2 w/w) film spun-cast from the solution (Fig. 4b). 2D GIXD

Table 1 Photovoltaic properties of the OPVs based on PTIPSBDT–DPP and $PC_{71}BM$ (1 : 2 w/w) under AM 1.5 G illumination (100 mW cm^{-2})

PTIPSBDT:DPP–$PC_{71}BM$ (1 : 2 w/w)	V_{oc} [V]	J_{sc} [mA cm^{-2}]	FF	PCE[a] [%]
1 vol% DIO	0.76	15.74	0.60	7.18 (7.01)
3 vol% DIO	0.76	16.21	0.65	8.00 (7.92)
5 vol% DIO	0.75	14.70	0.68	7.70 (7.54)

[a] Average PCE for five devices.

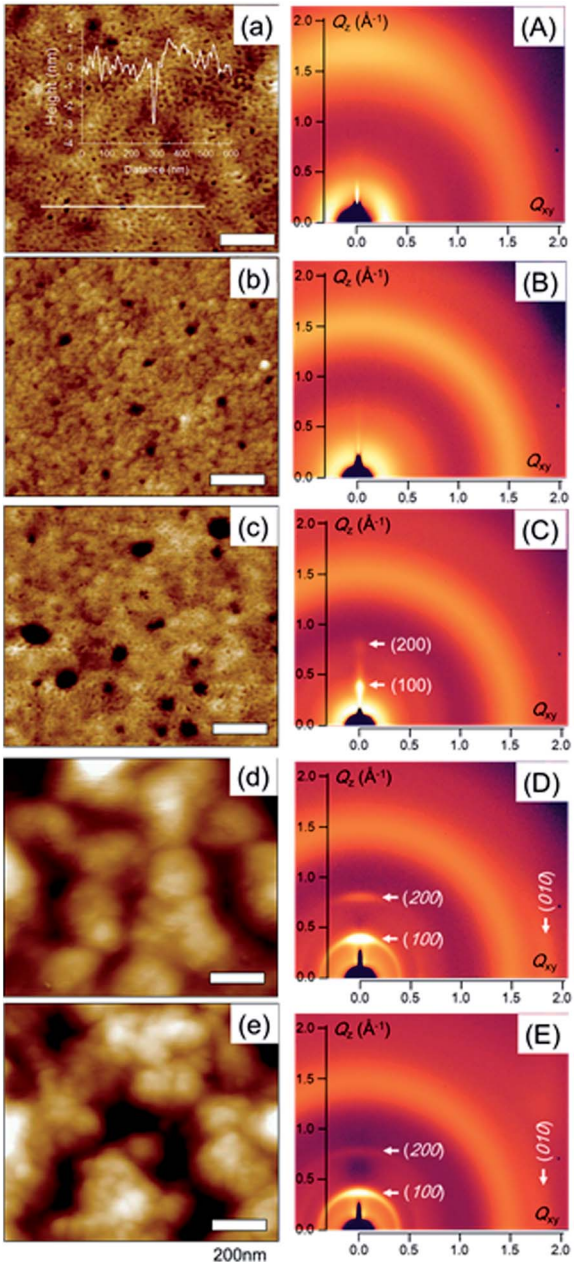

Fig. 4 2D-GIXD patterns and AFM image of spun-cast (a, A) PTIPSBDT–DPP and (b–e, B–E) PTIPSBDT–DPP:$PC_{71}BM$ (1 : 2 w/w) blend films with different DIO loadings: (b, B) 0 vol%; (c, C) 1 vol%; (d, D) 3 vol%; and (e, E) 5 vol% DIO.

patterns of these two films, showing only diffuse rings at both low and high Q values without any crystal diffraction, indicated amorphous-like PTIPSBDT–DPP and/or $PC_{71}BM$ structures in the as-spun films (Fig. 4A and B). In contrast, it was clear that the introduction of the DIO additive to the CB solvent had a positive effect on the segregation between the polymer and $PC_{71}BM$. As the DIO content was changed from 0 to 5 vol%, the phase separation between the miscible copolymer and $PC_{71}BM$ was accelerated, as easily indicated by an increase in the mean square surface roughness of the blend films: from 0.4 nm (for 0 vol%), to 1.16 nm, (for 1 vol%), 8.0 nm (for 3 vol%), and 12.6 nm (for 5 vol%) (Fig. 4c–e). TEM analysis also indicated a similar phase separation trend (Fig. S8 in the ESI†). Unlike the single CB solvent system, the 2D GIXD patterns of these DIO-assisted blend films showed typical X-ray reflections of the (h00) and (010) crystal planes along the Q_z (out-of-plane) and Q_{xy} (in-plane) axes, respectively, corresponding to PTIPSBDT–DPP crystals with intermolecular π-conjugation along the surface parallel direction (Fig. 4C–E). The layer spacings of (100) and (010), *i.e.*, $d_{(100)}$ and $d_{(010)}$, were indicated as 16.98 and 3.72 Å, respectively (Fig. S9 in the ESI†).

Interestingly, the $d_{(100)}$ value was well matched with the vertically stacked layer distance of TIPS-pentacene,[8,10] *i.e.*, 16.83 Å, in comparison to the DPP-based copolymers[11] with similar alkyl side chains (19.8–20.3 Å). Additionally, it was found that crystallinity in the PTIPSBDT–DPP was obtained at 3 vol% DIO (Fig. S9 in the ESI†); however, the anisotropic orientation of the π-conjugated planes, as determined by broad X-ray reflections along the Debye rings at given Q values, as indicated as the full width at half maximum (FWHM) at $Q_{(100)}$ (Fig. S10 in the ESI†): 9.8° (for 1 vol%), 21.1° (for 3 vol%), and 46.0° (for 5 vol%). The AFM and 2D GIXD results strongly supported the existence of an optimal loading of the DIO phase-separation promoter to induce a π-conjugated crystalline structure in the PTIPSBDT–DPP for high performance BHJ OPVs. In this study, the optimal DIO/CB binary solvent was obtained at 3 vol% DIO. The resulting spun-cast PTIPSBDT–DPP/$PC_{71}BM$ (1 : 2 w/w) blend films yielded the highest PCE values, up to 8%, in the OPVs, without any further treatment.

In conclusion, a new low band gap semiconducting polymer with high molecular weight, PTIPSBDT–DPP, was synthesized by Suzuki cross-coupling. PTIPSBDT–DPP showed a smaller band gap energy compared with similar BDT–DPP-based polymers due to the extended π-conjugation by the triple bonds in the TIPS units, and also a relatively deep HOMO energy level. PTIPSBDT–DPP showed an OFET hole mobility of up to 0.12 $cm^2\ V^{-1}\ s^{-1}$. These characteristics resulted in photovoltaic cells with high PCEs, up to 8.00%, when $PC_{71}BM$ was used as the electron acceptor.

Acknowledgements

This work was supported by a grant (no. 2012055225) from the Center for Advanced Soft Electronics under the Global Frontier Research Program of the Ministry of Education, Science and Technology, Korea, and a NRF grant funded by the Korea government (MSIP) through GCRC-SOP (no. 2011-0030013). H.Y. expresses thanks for the financial support provided under the Mid-career Research Program through the NRF (20110016177) funded by MEST.

Notes and references

1 (*a*) Y. Li, *Acc. Chem. Res.*, 2012, **45**, 723; (*b*) W. Li, K. H. Hendriks, W. S. C. Roelofs, Y. Kim, M. M. Wienk and R. A. J. Janssen, *Adv. Mater.*, 2013, **25**, 3182; (*c*) K. H. Hendriks, G. H. L. Heintges, V. S. Gevaerts, M. M. Wienk and R. A. J. Janssen, *Angew. Chem., Int. Ed.*,

2013, **52**, 1; (*d*) H. Zhou, L. Yang and W. You, *Macromolecules*, 2012, **45**, 607; (*e*) J. Peet, J. Y. Kim, N. E. Coates, W. L. Ma, D. Moses, A. J. Heeger and G. C. Bazan, *Nat. Mater.*, 2007, **6**, 497; (*f*) J. W. Chen and Y. Cao, *Acc. Chem. Res.*, 2009, **42**, 1709.

2 (*a*) J. Jo, J.-R. Pouliot, D. Wynands, S. D. Collins, J. Y. Kim, T. L. Nguyen, H. Y. Woo, Y. Sun, M. Leclerc and A. J. Heeger, *Adv. Mater.*, 2013, **25**, 4783; (*b*) J. S. Ha, K. H. Kim and D. H. Choi, *J. Am. Chem. Soc.*, 2011, **133**, 10364; (*c*) J.-H. Kim, C. E. Song, I.-N. Kang, W. S. Shin and D.-H. Hwang, *Chem. Commun.*, 2013, **49**, 3248; (*d*) M. Jφrgensen, K. Norrman, S. A. Gevorgyan, T. Tromholt, B. Andreasen and F. C. Krebs, *Adv. Mater.*, 2012, **24**, 580; (*e*) I. Meager, R. S. Ashraf, S. Rossbauer, H. Bronstein, J. E. Donaghey, J. Marshall, B. C. Schroeder, M. Heeney, T. D. Anthopoulos and I. McCulloch, *Macromolecules*, 2013, **46**, 5961.

3 (*a*) L. Dou, J. You, J. Yang, C.-C. Chen, Y. He, S. Murase, T. Moriarty, K. Emery, G. Li and Y. Yang, *Nat. Photonics*, 2012, **6**, 180; (*b*) L. Dou, W.-H. Chang, J. Gao, C.-C. Chen, J. You and Y. Yang, *Adv. Mater.*, 2013, **25**, 825; (*c*) L. Dou, J. Gao, E. Richard, J. You, C.-C. Chen, K. C. Cha, Y. He, G. Li and Y. Yang, *J. Am. Chem. Soc.*, 2012, **134**, 10071; (*d*) Q. Peng, Q. Huang, X. Hou, P. Chang, J. Xub and S. Deng, *Chem. Commun.*, 2012, **48**, 11452.

4 (*a*) J.-H. Kim, C. E. Song, H. U. Kim, A. C. Grimsdale, S.-J. Moon, W. S. Shin, S. K. Choi and D.-H. Hwang, *Chem. Mater.*, 2013, **25**, 2722; (*b*) J.-H. Kim, C. E. Song, N. Shin, H. Kang, S. Wood, I.-N. Kang, B. J. Kim, B. S. Kim, J.-S. Kim, W. S. Shin and D.-H. Hwang, *ACS Appl. Mater. Interfaces*, 2013, **5**, 12820.

5 Q. Shi, H. Fan, Y. Liu, W. Hu, Y. Li and X. Zhan, *Macromolecules*, 2011, **44**, 9173.

6 J.-K. Lee, M. C. Gwinner, R. Berger, C. Newby, R. Zentel, R. H. Friend, H. Sirringhaus and C. K. Ober, *J. Am. Chem. Soc.*, 2011, **133**, 9949.

7 J.-H. Kim, H. U. Kim, I.-N. Kang, S. K. Lee, S.-J. Moon, W. S. Shin and D.-H. Hwang, *Macromolecules*, 2012, **45**, 8628.

8 (*a*) M. Jang, J. H. Park, S. Im, S. H. Kim and H. Yang, *Adv. Mater.*, 2014, **26**, 288; (*b*) S. H. Kim, K. Hong, M. Jang, J. Jang, J. E. Anthony, H. Yang and C. E. Park, *Adv. Mater.*, 2010, **22**, 4809.

9 S. H. Kim, M. Jang, H. Yang, J. E. Anthony and C. E. Park, *Adv. Funct. Mater.*, 2011, **21**, 2198.

10 (*a*) J. E. Anthony, J. S. Brooks, D. L. Eaton and S. R. Parkin, *J. Am. Chem. Soc.*, 2001, **123**, 9482; (*b*) W. H. Lee, D. H. Kim, Y. Jang, J. H. Cho, M. Hwang, Y. D. Park, Y. H. Kim, J. I. Han and K. Cho, *Appl. Phys. Lett.*, 2007, **90**, 132106; (*c*) R. Hamilton, J. Smith, S. Ogier, M. Heeney, J. E. Anthony, I. McCulloch, J. Veres, D. D. C. Bradley and T. D. Anthopoulos, *Adv. Mater.*, 2009, **21**, 1166; (*d*) C. D. Sheraw, T. N. Jackson, D. L. Eaton and J. E. Anthony, *Adv. Mater.*, 2003, **15**, 2009; (*e*) Y. Diao, B. C.-K. Tee, G. Giri, J. Xu, D. H. Kim, H. A. Becerril, R. M. Stoltenberg, T. H. Lee, G. Xue, S. C. B. Mannsfeld and Z. Bao, *Nat. Mater.*, 2013, **12**, 665.

11 (*a*) J. W. Jung, J. W. Jo, F. Liu, T. P. Russell and W. H. Jo, *Chem. Commun.*, 2012, **48**, 6933; (*b*) P. Sonar, S. P. Singh, Y. Li, Z.-E. Ooi, T. Ha, I. Wong, M. S. Soh and A. Dodabalapur, *Energy Environ. Sci.*, 2011, **4**, 2288; (*c*) J. W. Jung, F. Liu, T. P. Russell and W. H. Jo, *Energy Environ. Sci.*, 2013, **6**, 3301.

